Pulsed X-Ray Detector Based on an Unintentionally-Doped High Resistivity ε-Ga_2O_3 Film

Jing Wang, Leidang Zhou, Xing Lu, Liang Chen, Zimin Chen, Xinbo Zou, *Member, IEEE*, Gang Wang, Boming Yang, and Xiaoping Ouyang

***Abstract*— Gallium Oxide (Ga_2O_3), an emerging ultra-wide band gap semiconductor, has drawn great attention for application in radiation detection. In this letter, ultrafast X-ray detectors have been fabricated using a high resistivity unintentionally-doped (UID) ε-Ga_2O_3 film grown on sapphire by metal-organic chemical vapor deposition (MOCVD). The detector featuring a lateral metal–semiconductor–metal (MSM) structure exhibited a low dark current < 2 nA at 100 V and its sensitivity was as high as 28.6 nC/Gy or ~1.0×10^6 nC/(Gy·cm^3) at 40 V and an X-ray dose rate of 0.383 Gy/s. A stable and repeatable transient response was observed for the detectors under switching X-ray illumination. Furthermore, the detector achieved a pulsed X-ray detection with 50 ns in full width and its time resolution was revealed to be ~7.1 ns. These results imply the great potential of the MOCVD-grown high-resistivity UID ε-Ga_2O_3 film for ultrafast X-ray detection.**

***Index Terms*— Ga_2O_3 film, X-ray detection, semiconductor radiation detector, pulsed measurement.**

I. Introduction

GALLIUM Oxide (Ga_2O_3), which possesses a wide direct band gap of ~ 4.9 eV, a high critical electric field of 8 MV/cm and an excellent tolerance to irradiation, is a promising material for X-ray and high-energy particle detection applications [1], [2], [3]. Previously, Lu et al. demonstrated the first β-Ga_2O_3 Schottky X-ray detectors based on a single crystalline bulk substrate [4]. Later, various types of Ga_2O_3 X-ray detectors have been developed based on either single crystals or polycrystalline/amorphous thin films [5], [6], [7], [8], [9], [10], [11], [12]. Compared to polycrystalline/amorphous material, the single crystals material with low defects will ensure both fast response and high sensitivity of the detector [13], [14].

Usually, the unintentionally-doped (UID) Ga_2O_3 single crystals show an n-type conductivity, which are not suitable for fabricating metal–semiconductor–metal (MSM) detectors due to a high dark current issue. Very recently, pulsed X-ray detectors with a nanosecond time resolution have been realized using a Fe doped high resistivity β-Ga_2O_3 single crystal substrate [9], in which Fe was adopted as deep acceptors to compensate the background n-type conductivity in the material. However, the compensation doping would inevitably deteriorate the crystalline quality and produce defects within the Ga_2O_3 lattice, bringing some adverse effects to the performance of the detector, for example decreasing its sensitivity. Moreover, the β-Ga_2O_3 single crystal substrates at current stage are of small size and still too expensive from a commercial point of view.

On the other hand, high quality single crystalline ε-Ga_2O_3 films have been successfully grown on low cost sapphire substrates by metal-organic chemical vapor deposition (MOCVD) [15], [16], [17], [18]. Featuring an intrinsic high resistivity, the MSM X-ray detectors based on a hetero-epitaxial UID ε-Ga_2O_3 film demonstrated a remarkably high sensitivity [12], which suggested a great potential in reducing the production cost while maintaining a high performance for future X-ray detection applications.

In this study, based on an MOCVD-grown high resistivity UID ε-Ga_2O_3 film, a MSM detector was fabricated and characterized for pulsed X-ray detection. The detector achieved a 50 ns in full width pulsed X-ray measurement and its time resolution was revealed to be ~ 7.1 ns.

II. Experiments

The MSM detector was fabricated using UID ε-Ga_2O_3 thin film grown on sapphire substrate by MOCVD. More detailed information about the epitaxy process could be found in our previous reports [15], [19]. The Al interdigital electrodes were deposited on top of the ε-Ga_2O_3 film by E-beam evaporation, and the distance between the neighboring electrodes was 0.5 mm.

Manuscript received 18 October 2022; revised 17 November 2022; accepted 19 November 2022. Date of publication 23 November 2022; date of current version 7 December 2022. This work was supported in part by the Guangdong Basic and Applied Basic Research Foundation under Grant 2022A1515012163 and in part by the National Natural Science Foundation of China under Grant 62204198. *(Corresponding author: Leidang Zhou.)*

Jing Wang is with the School of Microelectronics, Xidian University, Xi'an 710071, China, and also with the Northwest Institute of Nuclear Technology, Xi'an 710024, China.

Leidang Zhou is with the State Key Laboratory of Multiphase Flow in Power Engineering and the School of Microelectronics, Xi'an Jiaotong University, Xi'an 710049, China (e-mail: zhould@xjtu.edu.cn).

Xing Lu, Zimin Chen, and Gang Wang are with the State Key Laboratory of Optoelectronic Materials and Technologies, School of Electronics and Information Technology, Sun Yat-sen University, Guangzhou 510275, China (e-mail: lux86@mail.sysu.edu.cn).

Liang Chen and Xiaoping Ouyang are with the Radiation Detection Research Center, Northwest Institute of Nuclear Technology, Xi'an 710024, China.

Xinbo Zou is with the School of Information Science and Technology, ShanghaiTech University, Shanghai 201210, China.

Boming Yang is with the School of Microelectronics, Xi'an Jiaotong University, Xi'an 710049, China.

Color versions of one or more figures in this letter are available at https://doi.org/10.1109/LPT.2022.3224014.

Digital Object Identifier 10.1109/LPT.2022.3224014

1041-1135 © 2022 IEEE. Personal use is permitted, but republication/redistribution requires IEEE permission.
See https://www.ieee.org/publications/rights/index.html for more information.

Authorized licensed use limited to: ShanghaiTech University. Downloaded on January 04,2024 at 14:56:47 UTC from IEEE Xplore. Restrictions apply.

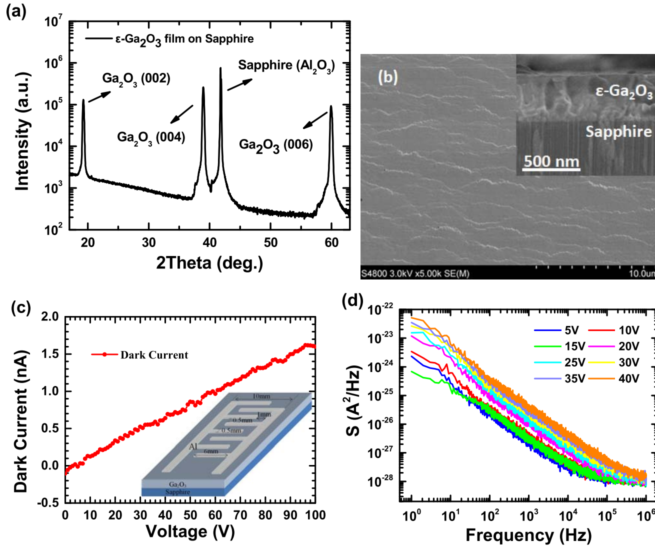

Fig. 1. (a) The XRD pattern and (b) The plan-view SEM image of the ε-Ga_2O_3 film grown on a sapphire substrate. (c) The typical dark I-V characteristics of the fabricated ε-Ga_2O_3 detector. Insert shows the structure of detector. (d) The LFN equivalent spectra at different bias voltages.

A test unit (Agilent B2902A) was used for measuring the I-V characteristics. The low frequency noise (LFN) analysis was performed to figure out the influence of defects on the carrier transport process in the detectors.

The X-ray source used in this study was an X-ray tube with a tungsten anode, which operated at the tube currents between 1 μA and 400 μA and a tube voltage of 30 kV with the corresponding X-ray dose rates ranging from 3.83 mGy/s to 1.532 Gy/s and proportional to the tube current. The maximum X-ray photon energy was 30 keV and the X-ray beam was perpendicularly illuminated to the ε-Ga_2O_3 detector in all the measurements. An XRS-4 pulsed X-ray source with 50 ns in full width was used for the pulsed X-ray detection test and the response signal was recorded by an oscilloscope from a 50-Ω resistor, which was connected in series with the detector.

III. Results and Discussion

Fig.1 (a) shows the X-ray diffraction (XRD) pattern of the as-grown ε-Ga_2O_3 sample. Three peaks at 19.284°, 38.964° and 59.924° were attributed to the (002), (004) and (004) planes of the ε-Ga_2O_3 film, while the peak at 41.784° corresponded the sapphire (Al_2O_3) substrate. The full width at halfmaximum (FWHM) of the rocking curve of the (004) diffraction peak of ε-Ga_2O_3 was 0.1728° (622″), which confirmed that a high quality phase-pure single-crystalline ε-Ga_2O_3 film was achieved in our study [15], [19], [20], [21]. The plan-view scanning electron microscopy (SEM) image in Fig.1 (b) shows a high crystallinity of the heteroepitaxial ε-Ga_2O_3 film without obvious grain boundary. The inset shows the cross section of the fabricated film, and the thickness of the film was 380 nm. Fig.1 (c) shows the device structure of the fabricated ε-Ga_2O_3 MSM detector and its typical I-V characteristic under dark condition. The dark current of the detector remained below 2 nA at a bias of 100 V, indicating that the epitaxial UID ε-Ga_2O_3 film in our study had an intrinsic high resistivity. Unlike the reported Ga_2O_3 detectors based on the Fe/Mg compensation doped material [6], [7], [8], [9], the intrinsic high resistivity property of the UID ε-Ga_2O_3 film would keep the carrier transport process of the detector far from the influence of defects. Fig.1 (d) shows the LFN spectra of the detector at various bias voltages. The measured curves can be represented as the function of $1/f$ and a weak generation-recombination (GR) noise appended at 10 Hz. When the bias voltage was increased from 5 V to 40 V, the measured noise of our detector kept in the same tendency and merely grew from 1×10^{-24} (A^2/Hz) to 1×10^{-23} (A^2/Hz), which were close to the system noise below 10^{-26} (A^2/Hz). Thereby, the noise level of detector was quite low and weakly dependent on the bias voltage, and the device was not seriously affected by the defects [22], [23].

Fig.2 (a) shows the response net currents ($I_{X-ray} - I_{dark}$) of the detector to the X-ray illumination with different X-ray tube current as a function of bias voltage. Obviously, the net current of the detector increased with both the X-ray dose rates and the bias voltage. The unsaturated net current against bias voltage indicated an incomplete collection of the radiation-generated carriers in our detector. According to the Hecht equation [24], the efficiency of carrier collection could be increased by enlarging the electric field between the electrodes (E) for an MSM detector and it would eventually get saturated when E went strong enough. In this case, the response of the detector could be further enhanced.

The sensitivity of the detector is defined as the ratio between the net current and the incident X-ray dose rate reaching to the detector (D):

$$\text{Sensitivity} = \frac{\text{Net Current}}{D} = \frac{I_{\text{X-ray}} - I_{\text{dark}}}{D} \tag{1}$$

When the X-ray tube current was set at 100 μA, the net current of the detector biased at 40 V was 11 nA (23 nA @100 V) and the X-ray dose rate reaching to the detector was calibrated to be 0.383 Gy/s. Therefore, the sensitivity was calculated to be 28.6 nC/Gy (60 nC/Gy @100 V). In order to make a comparison with our previous studies under the same X-ray illumination ($D = 0.383$ Gy/s) and bias condition ($E = 800$ V/cm @40 V), the normalized sensitivity to device active volume was calculated according to:

$$\text{Normalized Sensitivity} = \frac{\text{Sensitivity}}{\text{Device active Volume}} \tag{2}$$

The normalized sensitivity of the ε-Ga_2O_3 detector in this study was as high as $\sim 1.0 \times 10^6$ nC/(Gy · cm^3), which was much higher than that of a high-resistivity polycrystalline ZnO detector $\sim 1.1 \times 10^5$ nC/(Gy · cm^3) [25] and a Fe-doped high-resistivity single crystalline β-Ga_2O_3 detector $\sim 2.2 \times 10^1$ nC/(Gy·cm^3) [9]. The higher normalized sensitivity in this study could be mainly attributed to the low defects density in the UID ε-Ga_2O_3 epitaxial film.

The net current and sensitivity of the detector biased at −40 V and −100 V are plotted as a function of the X-ray dose rate in Fig. 2(b). The device showed a nonlinear output with a reduced sensitivity at higher X-ray dose rate, which indicated that the carrier collection efficiency degraded when the X-ray dose rate increased. According to the band-to-band

Authorized licensed use limited to: ShanghaiTech University. Downloaded on January 04,2024 at 14:56:47 UTC from IEEE Xplore. Restrictions apply.

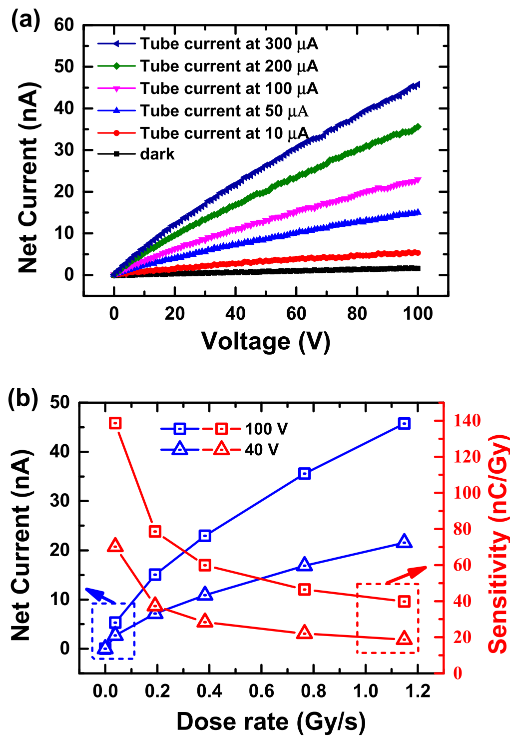

Fig. 2. (a) The net current of the detector at various X-ray tube currents as a function of the bias voltage. (b) The net current and sensitivity of the detector biased at −40 V and −100 V as a function of X-ray dose rate.

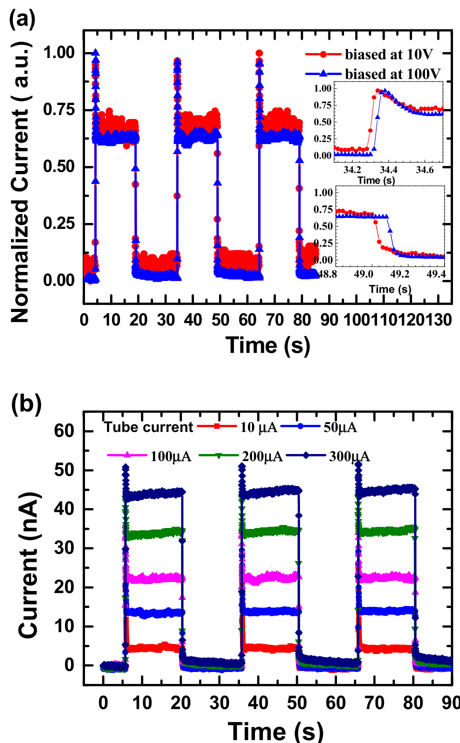

Fig. 3. The transient responses of the ε-Ga_2O_3 detector under (a) different bias voltages and (b) different X-ray dose rates.

recombination theory, the recombination rate of the radiation-generated carriers increased with the increase of the carrier density, which was directly proportional to the incident X-ray dose rate. However, the collection of the radiation-generated carriers in our detector was incomplete.

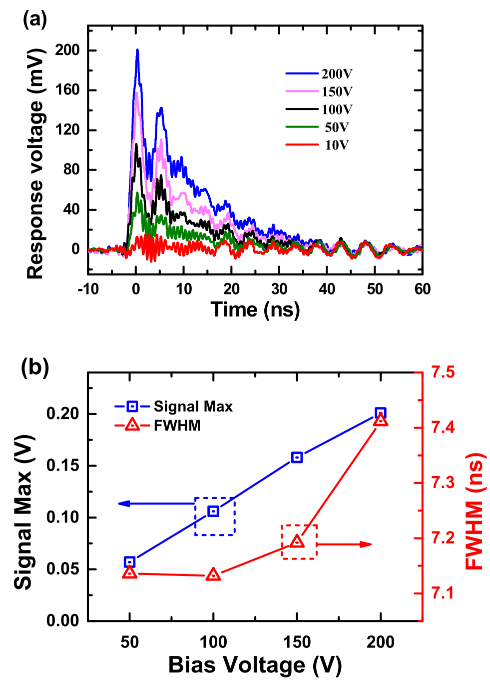

Fig. 4. (a) The pulsed X-ray responses of the fabricated ε-Ga_2O_3 detector at various bias voltages. (b) The maximal amplitude and FWHM of response signals.

Owing to the intrinsic high resistivity property of the UID ε-Ga_2O_3 film, the fabricated detector was expected to exhibit a fast response to the X-ray illumination. Fig.3 (a) and (b) show the transient responses of the ε-Ga_2O_3 detector under different bias voltages and different X-ray dose rates, respectively. The X-ray switching period was set to be 30 s and the sampling interval of the measurement was 20 ms. It was revealed that the detector exhibited a good and stable transient response with both the rise time (10% to 90%) and decay time (90% to 10%) of less than 50 ms, as shown by the enlarged plot of the rise and decay process in the inset of Fig. 3 (a).

The pulsed X-ray response of the fabricated ε-Ga_2O_3 detector was characterized using an XRS-4 pulsed X-ray source and the response signals at various bias voltages were shown in Fig. 4 (a). The ε-Ga_2O_3 detector exhibited an obvious pulsed response to the 50 ns in full width pulsed X-ray illumination when the bias voltage was larger than 50V, while it was hardly distinguished at a bias voltage of 10 V due the low signal-to-noise ratio (SNR). The maximum amplitude and the full width at half maxima (FWHM) of the response signals were plotted as a function of bias voltages in Fig. 4(b). The maximum value of the response signal increased linearly with the bias voltage, which was attributed to the incomplete carrier collection efficiency of the detector as discussed before. A time resolution of $\sim$ 7.1 ns was determined by the FHWM of the pulsed response signal when the detector was biased at 100 V, which was in the same level with the previously reported Fe-doped β-Ga_2O_3 detector [9]. Compared to the polycrystalline ZnO detector in [23], which was in the same device topology but had a millisecond time resolution, the ε-Ga_2O_3 detector in this study showed a much faster response by three orders of magnitude. Owing to the single crystalline and intrinsic high resistivity properties of the epitaxial ε-Ga_2O_3

Authorized licensed use limited to: ShanghaiTech University. Downloaded on January 04,2024 at 14:56:47 UTC from IEEE Xplore. Restrictions apply.

TABLE I
COMPARISON OF PERFORMANCE X-RAY DETECTORS BASED ON WIDE GAP SEMICONDUCTORS

Detectors	Sensitivity / $C \cdot Gy^{-1} \cdot cm^{-3}$	Rise/Fall time /s	Pulsed response
GaN p-i-n[26]	3.4×10^{-4}@0V	< 20 m	N/A
Ni/GaN:Fe/Ti (bulk)[27]	N/A	28	N/A
Al/ZnO/Al (p.film)[25]	1.1×10^{-4}@40V	< 0.2	1 ms
Pt/Diamond/Pt (film)[28]	5.8×10^{-2}@150V	0.008	N/A
Ti/β-Ga_2O_3:Mg/Ti (bulk)[7]	3×10^{-3}@1000V	< 0.2	N/A
Ti/β-Ga_2O_3:Fe/Ti (bulk)[9]	2.2×10^{-8}@40V	0.02	< 2 ns
ITO/Ga_2O_3/ITO (a.film)[10]	0.271@50V	68.3/51.3	N/A
Au/α-Ga_2O_3/Au (n.film)[11]	0.1388@50V	< 0.035	N/A
Au/ε-Ga_2O_3/Au (film)[12]	4.75×10^{3}@20V	132/37 m	N/A
This work (film)	1.0×10^{-3}@40V	< 0.05	< 7.1 ns

Notes: p.film means polycrystalline film; a.film means amorphous film; n.film means nanocrystalline film.

film, the carrier transport process in the detector would be less affected by defects.

The time resolution of the detector might be faster than 7.1 ns actually, limited by the pulsed source in the experiment. Because the detector exhibited the 50 ns pulsed waveform in the same width with the XRS-4 pulsed X-ray source and the FWHM had reached 7.1 ns beyond 50 V bias voltage. What's more, XRS-4 pulsed X-ray source was a multi-peak source, some pulsed peaks can be detectable with the increase of the sensitivity of the detector. Thereby, the FWHM of the envelopment of the pulsed response curve just slightly grew with the bias voltage beyond 100 V.

Table I shows the comparison of the normalized sensitivity and response speed of our device with various reported detectors using wide band gap semiconductors. The result clearly indicates that the low cost UID ε-Ga_2O_3 film based detector has great potential in fast X-ray radiation detection.

IV. CONCLUSION

In summary, a single crystalline UID ε-Ga_2O_3 film was grown on a sapphire substrate by MOCVD and fabricated into an MSM X-ray detector. Featuring an intrinsic high resistivity property of the ε-Ga_2O_3 epilayer, the detector exhibited a low dark current and a relatively high sensitivity. Pulsed X-ray detection with a time resolution of $\sim$ 7.1 ns was demonstrated using the fabricated ε-Ga_2O_3 detector.

REFERENCES

[1] S. J. Pearton et al., "A review of Ga_2O_3 materials, processing, and devices," *Appl. Phys. Rev.*, vol. 5, no. 1, 2018, Art. no. 011301, doi: 10.1063/1.5006941.

[2] J. Kim et al., "Radiation damage effects in Ga_2O_3 materials and devices," *J. Mater. Chem. C*, vol. 7, no. 1, pp. 10–24, 2019, doi: 10.1039/C8TC04193H.

[3] D. Szalkai et al., "β-Ga_2O_3 solid-state devices for fast neutron detection," *IEEE Trans. Nucl. Sci.*, vol. 64, no. 6, pp. 1574–1579, Jun. 2017, doi: 10.1109/TNS.2017.2698831.

[4] X. Lu et al., "Schottky X-ray detectors based on a bulk β-Ga_2O_3 substrate," *Appl. Phys. Lett.*, vol. 112, no. 10, 2018, Art. no. 103502, doi: 10.1063/1.5020178.

[5] X. Lu et al., "X-ray detection performance of vertical Schottky photodiodes based on a bulk β-Ga_2O_3 substrate grown by an EFG method," *ECS J. Solid State Sci. Technol.*, vol. 8, no. 7, pp. Q3046–Q3049, 2019, doi: 10.1149/2.0071907jss.

[6] I. Hany, G. Yang, and C. C. Chung, "Fast X-ray detectors based on bulk β-Ga_2O_3 (Fe)," *J. Mater. Sci.*, vol. 55, no. 22, pp. 9461–9469, 2020, doi: 10.1007/s10853-020-04665-9.

[7] J. W. Chen et al., "High-performance X-ray detector based on single-crystal β-Ga_2O_3:Mg," *ACS Appl. Mater. Interfaces*, vol. 13, no. 2, pp. 2879–2886, 2021, doi: 10.1021/acsami.0c20574.

[8] J. W. Chen et al., "Highly sensitive X-ray detector based on a β-Ga_2O_3:Fe single crystal," *Opt. Exp.*, vol. 29, no. 15, pp. 23292–23299, 2021, doi: 10.1364/OE.435366.

[9] L. D. Zhou et al., "Pulsed X-ray detector based on Fe doped β-Ga_2O_3 single crystal," *J. Phys. D, Appl. Phys.*, vol. 54, no. 27, 2021, Art. no. 274001, doi: 10.1088/1361-6463/abf53b.

[10] H. Liang et al., "Detectors based on amorphous Ga_2O_3 thin films," *ACS Photon.*, vol. 6, no. 2, pp. 351–359, 2018, doi: 10.1021/acsphotonics.8b00769.

[11] M. N. Chen et al., "Fast-response X-ray detector based on nanocrystalline Ga_2O_3 thin film prepared at room temperature," *Appl. Surf. Sci.*, vol. 554, 2021, Art. no. 149619, doi: 10.1016/j.apsusc.2021.149619.

[12] Z. P. Zhang et al., "ε-Ga_2O_3 thin film avalanche low-energy X-ray detectors for highly sensitive detection and fast-response applications," *Adv. Mater. Technol.*, vol. 6, no. 4, 2021, Art. no. 2001094, doi: 10.1002/admt.202001094.

[13] A. Mirzaei, J.-S. Huh, S. S. Kim, and H. W. Kim, "Room temperature hard radiation detectors based on solid state compound semiconductors: An overview," *Electron. Mater. Lett.*, vol. 14, no. 3, pp. 261–287, May 2018, doi: 10.1007/s13391-018-0033-2.

[14] P. M. Johns and J. C. Nino, "Room temperature semiconductor detectors for nuclear security," *J. Appl. Phys.*, vol. 126, no. 4, Jul. 2019, Art. no. 040902, doi: 10.1063/1.5091805.

[15] Z. M. Chen et al., "Layer-by-layer growth of ε-Ga_2O_3 thin film by metal–organic chemical vapor deposition," *Appl. Phys. Exp.*, vol. 11, no. 10, 2018, Art. no. 101101, doi: 10.7567/APEX.11.101101.

[16] Z. Chen et al., "ε-Ga_2O_3: An emerging wide bandgap piezoelectric semiconductor for application in radio frequency resonators," *Adv. Sci.*, vol. 9, no. 32, 2022, Art. no. 2203927, doi: 10.1002/advs.202203927.

[17] F. Boschi et al., "Hetero-epitaxy of ε-Ga_2O_3 layers by MOCVD and ALD," *J. Cryst. Growth*, vol. 443, pp. 25–30, Jun. 2016, doi: 10.1016/j.jcrysgro.2016.03.013.

[18] F. Mezzadri et al., "Crystal structure and ferroelectric properties of ε-Ga_2O_3 films grown on (0001)-sapphire," *Inorganic Chem.*, vol. 55, no. 22, 2016, 12079–12084, doi: 10.1021/acs.inorgchem.6b02244.

[19] W. Chen, H. Luo, Z. Chen, Y. Pei, G. Wang, and X. Lu, "First demonstration of hetero-epitaxial ε-Ga_2O_3 MOSFETs by MOCVD and a F-plasma surface doping," *Appl. Surf. Sci.*, vol. 603, Nov. 2022, Art. no. 154440, doi: 10.1016/j.apsusc.2022.154440.

[20] H. Sun et al., "HCl flow-induced phase change of α-, β-, and ε-Ga_2O_3 films grown by MOCVD," *Cryst. Growth Des.*, vol. 18, no. 4, pp. 2370–2376, 2018, doi: 10.1021/acs.cgd.7b01791.

[21] Y. Qin et al., "Metal–semiconductor–metal ε-Ga_2O_3 solar-blind photodetectors with a record-high responsivity rejection ratio and their gain mechanism," *ACS Photon.*, vol. 7, no. 3, pp. 812–820, 2020, doi: 10.1021/acsphotonics.9b01727.

[22] S. Beyne, O. V. Pedreira, I. D. Wolf, Z. Tőkei, and K. Croes, "A novel electromigration characterization method based on low-frequency noise measurements," *Semicond. Sci. Technol.*, vol. 34, no. 7, Jul. 2019, Art. no. 075002, doi: 10.1088/1361-6641/ab1963.

[23] Q. Shen et al., "Characterization of low-frequency excess noise in $CH_3NH_3PbI_3$-based solar cells grown by solution and hybrid chemical vapor deposition techniques," *ACS Appl. Mater. Interfaces*, vol. 10, no. 1, pp. 371–380, 2017, doi: 10.1021/acsami.7b10091.

[24] M. B. H. Breese, E. Vittone, G. Vizkelethy, and P. J. Sellin, "A review of ion beam induced charge microscopy," *Nucl. Instrum. Methods Phys. Res. B, Beam Interact. Mater. At.*, vol. 264, no. 2, pp. 345–360, Nov. 2007, doi: 10.1016/j.nimb.2007.09.031.

[25] L. D. Zhou et al., "A high-resistivity ZnO film-based photoconductive X-ray detector," *IEEE Photon. Technol. Lett.*, vol. 31, no. 5, pp. 365–368, Mar. 1, 2019, doi: 10.1109/LPT.2019.2894296.

[26] L. D. Zhou et al., "Self-powered fast-response X-ray detectors based on vertical GaN p-n diodes," *IEEE Electron Device Lett.*, vol. 40, no. 7, pp. 1044–1047, Jul. 2019, doi: 10.1109/LED.2019.2914585.

[27] K. Fu, G. Yu, C. Yao, G. Wang, M. Lu, and G. Zhang, "X-ray detectors based on Fe doped GaN photoconductors," *Phys. Status Solidi-Rapid Res. Lett.*, vol. 5, nos. 5–6, pp. 187–189, 2011, doi: 10.1002/pssr.201105163.

[28] D. M. Trucchi, P. Allegrini, P. Calvani, A. Galbiati, K. Oliver, and G. Conte, "Very fast and primingless single-crystal-diamond X-ray dosimeters," *IEEE Electron Device Lett.*, vol. 33, no. 4, pp. 615–617, Apr. 2012, doi: 10.1109/LED.2012.2185476.

Authorized licensed use limited to: ShanghaiTech University. Downloaded on January 04,2024 at 14:56:47 UTC from IEEE Xplore. Restrictions apply.